Digital PCR detection of *Mycobacterium tuberculosis* and HIV-1 co-localization in spinal tuberculosis biopsies

Authors:

Robyn Waters[1,2,*], Adrian R Martineau[3], Maritz Laubscher[1], Robert N Dunn[1], Michael Held[1], Melissa-Rose Abrahams[2,4,#], Anna K Coussens[2,5,6,7,#,*]

Author affiliations:

[1]Division of Orthopaedic Surgery, Department of Surgery, Faculty of Health Sciences, University of Cape Town, South Africa.

[2]Wellcome Discovery Platforms in Infection, Institute of Infectious Disease and Molecular Medicine, Faculty of Health Sciences, University of Cape Town, South Africa.

[3]Centre for Immunobiology, Blizard Institute, Faculty of Medicine and Dentistry, Queen Mary University of London.

[4]Division of Medical Virology, Department of Pathology, Institute of Infectious Disease and Molecular Medicine, Faculty of Health Sciences, University of Cape Town, South Africa.

[5]Infectious Diseases and Immune Defence Division, Walter and Eliza Hall Institute of Medical Research (WEHI), Parkville, Victoria, Australia.

[6]Division of Medical Microbiology, Department of Pathology, Faculty of Health Sciences, University of Cape Town, South Africa.

[7]Department of Medical Biology (WEHI), Faculty of Medicine, Dentistry and Health Sciences, University of Melbourne, Parkville, Victoria, Australia.

[#]Equal contribution

*Co-corresponding authors

Contacts:

Anna Coussens, Walter and Eliza Hall Institute of Medical Research (WEHI), 1G Royal Parade, Parkville, 3052, Australia; Tel: +61 3 39452699; Email: coussens.a@wehi.edu.au

Robyn Waters, Division of Orthopaedic Surgery, University of Cape Town, Anzio Rd, Observatory, 7925, South Africa; Email: robyn.waters@uct.ac.za

ABSTRACT

Background. The paucibacillary nature of spinal tuberculosis (STB) makes diagnosis challenging, particularly in people living with HIV-1 (PLWH). It is suggested that HIV-1 and *Mycobacterium tuberculosis* (*Mtb*) co-infection in tissues favours reciprocal replication, infection and reservoir expansion. Yet, confirmation of this detrimental synergism in diseased tissues is scant.

Methods. In a prospective study of 25 adults (13 (52%) people living with HIV-1 (PLWH) on antiretroviral treatment (ART)) undergoing spinal biopsy investigation for STB in South Africa, droplet digital PCR (ddPCR) was used to detect and quantify *Mtb* complex (MTBC) DNA (*rpoB* and *IS6110*) in 93 biopsy segments, and HIV-1 DNA (*pol* and *gag*) in 41 segments from PLWH. ddPCR sensitivity for *Mtb* was validated against Xpert-Ultra and culture. Relationships between pathogen DNA abundance, co-detection, human cellularity, HIV status, and peripheral viral load (VL) were evaluated.

Findings. ddPCR detected MTBC DNA in 19/25 (76%) patients (range: 8-59,144 *rpoB* copies/biopsy), with increased detection in those with confirmed STB and a history of TB. MTBC *rpoB* copies/million cells were higher in biopsies from PLWH (p=0.0096) and positively correlated with matched biopsy segment HIV-1 *pol* copies/million cells (r=0.40; p=0.0003), but not peripheral VL. HIV-1 DNA was detected in all biopsies from PLWH, four with undetectable VL. HIV-1 *pol* copies/million cells were higher in biopsy segments with MTBC DNA co-detected (p=0.011) and strongly correlated with VL (r=0.91; p=0.0003).

Interpretation. ddPCR has high sensitivity for *Mtb* and HIV-1 DNA quantification in STB biopsies. *Mtb* tissue abundance correlated with localised but not systemic HIV-1 abundance. Increased HIV-1 DNA detection at sites co-localised with *Mtb* supports further investigating the TB microenvironment as a site for HIV-1 reservoir persistence and expansion in PLWH on ART.

52 **Funding.** Wellcome (203135Z/16/Z); Academy of Science of SA (ASSAf); ORU, UCT; UCT
53 Merit Award.

54 **Keywords**: ddPCR, diagnostic, *Mtb*, TB-HIV co-infection, HIV reservoir, biopsy.

55

56 **INTRODUCTION**

57 In persons living with HIV (PLWH), the presence of HIV-1 co-infection can complicate the
58 diagnosis of tuberculosis (TB), with atypical radiographic findings, reduced sensitivity of
59 diagnostic tools[1], and TB often manifesting in extrapulmonary sites which are difficult to access
60 without invasive procedures.[2] In South Africa (SA), TB-HIV coinfection rates are high, and
61 development of tuberculosis in the spine (STB) is one of the most common EPTB sites in PLWH.[3-
62 6] *Mycobacterium tuberculosis* (*Mtb*) infection of the spine, and associated inflammatory damage
63 to the spinal architecture, is painful and debilitating. Rapid diagnosis on biopsy, using highly
64 sensitive techniques, and prompt initiation of anti-tuberculous treatment, are crucial to reduce
65 morbidity and life-long disability in STB patients.[4, 7-11]

66

67 The utility of digital droplet PCR (ddPCR) to detect *Mtb* in clinical samples has recently been
68 demonstrated using DNA derived from whole blood and formalin-fixed and paraffin-embedded
69 (FFPE) samples from EP sites[12-16], although utility for the specific detection of *Mtb* in bone and
70 joint biopsy samples has yet to be explored. Recent findings in CD34+ stem cells from the whole
71 blood of healthy individuals have implicated the bone marrow as a potential niche for *Mtb*
72 infection, with MTBC DNA more frequently detected by ddPCR in circulating CD34+ cells than
73 CD34-, with increased MTBC DNA detection in PLWH.[16] The bone marrow, as a deep anatomical
74 tissue site, has also been implicated as a viral tissue reservoir that enables the persistence of HIV-
75 1 infection in PLWH on ART[17], although much remains unclear about the mechanisms of this
76 persistence. HIV reservoir quantification is essential for evaluating efficacy of HIV cure
77 strategies. Multiplexed ddPCR assays also provide the unique opportunity to quantitate the HIV-
78 1 reservoir, ensuring sensitive, and specific quantification of viral genomes from multiple HIV-1
79 subtypes including subtype C, which dominates in SA and globally, and may thus provide valuable

80 insights into tissue reservoir dynamics following initiation of ART[18-21] and the impact of and on
81 tissue co-localised *Mtb* infection.
82
83 We and others have previously hypothesized that not only may active HIV-1 infection increase
84 *Mtb* replication at co-infection sites precipitating TB development, but that the inflammatory tissue
85 microenvironment at the site of *Mtb* infection may reciprocally increase HIV-1 reservoir size and
86 activation, by driving viral replication and increasing the pool of infection susceptible cells. Such
87 a relationship may be particularly evident when TB develops within an HIV-1
88 sanctuary/anatomical reservoir site.[22, 23] Counter to the often paucibacillary nature of pulmonary
89 TB (PTB), in PLWH, we recently found PLWH on ART had no significant difference in spinal
90 biopsy total *Mtb* abundance, using surrogate measures of time to culture positivity or Xpert
91 MTB/RIF Ultra cycle threshold (Ct), compared to HIV-1 uninfected patients.[24] We also found
92 Xpert MTB/RIF Ultra to have a higher sensitivity than culture in detecting *Mtb* in both open and
93 percutaneous CT-guided biopsies.[24]
94
95 The aim of this study was therefore to optimize and evaluate the utility of ddPCR to detect and
96 accurately quantify *Mtb* and HIV-1 DNA in both open and percutaneous CT-guided spinal biopsy
97 tissue, to determine i) if ddPCR is more sensitive than clinically validated tools for *Mtb* detection
98 in STB biopsies, ii) if HIV-1 proviral DNA can be detected at the site of spinal TB in ART
99 established PLWH, iii) if tissue localised presence and/or abundance of HIV-1 associates with *Mtb*
100 abundance in spinal tissues, and iv) whether peripheral HIV-1 viral load (VL) is associated with
101 spinal tissue *Mtb* and/or HIV-1 abundance.

102 **METHODS**

103 **Study design**

104 This is a sub-study of a prospective, longitudinal, observational cohort previously described.[24]
105 Adults (>18 years) with suspected STB were recruited at Groote Schuur Hospital, a public hospital
106 servicing a population of low socio-economic backgrounds, and low-income households in
107 densely populated vulnerable communities in Cape Town, South Africa, between November 2020
108 and December 2021. Based on diagnostic results of Xpert MTB/RIF Ultra (GXPU), MGIT TB
109 culture (TBCUL) and histology/histopathology (HIST) from the main study[24], patients were
110 divided into three groups: *Culture-confirmed STB* (TBCUL+GXPU+HIST+), *Xpert Ultra-*
111 *confirmed STB* (TBCUL-GXPU+HIST+), *Not STB* (TBCUL-GXPU-HIST-, alternate diagnosis
112 Supplemental Table S1).

113 **Study Approval**

114 The study was approved by the Human Research Ethics Committee, University of Cape Town
115 (HREC 606/2019). Written informed consent was obtained from all patients.

116 **Study procedures**

117 Clinical data were collected as previously described[24] and detailed in Supplemental Methods.
118 Spinal biopsy samples were collected via percutaneous CT-guided biopsy or open biopsy in
119 theatre, as previously described.[24] Tissues were immediately submerged in DNA/RNA Shield™
120 (Zymo Research, diluted 1:1 nuclease-free water (Sigma)), maintained at 4°C overnight, and stored
121 at -80°C . Tissue homogenization workflow, DNA extraction and quantification is detailed in
122 Supplemental Methods and Supplemental Figure S1. Briefly, after thawing, larger open biopsies

123 were cut into four equal sized tissue segments measuring approximately 1 cm^2 each homogenized
124 independently for DNA extraction (Supplemental Figure S2). A fifth sample comprising of
125 combined left-over biopsy homogenate from each of the four segments was also prepared for a
126 separate DNA extraction. Small CT-guided biopsy cores, ranging from 2-7 mm long by 1 mm
127 wide, were used in their entirety as a single sample (Supplemental Figure S3).

128 Three separate ddPCR reactions were prepared for the detection of MTBC (duplex: *rpoB* and
129 *IS6110*), HIV-1 (duplex: *pol* and *gag*) and human housekeeping gene ribonuclease P protein
130 subunit p30 (single-plex: *RPP30*) using a total of 1 µg total DNA each for MTBC and HIV-1
131 assays and 100 ng for the *RPP30* assay. The inclusion of two *Mtb* targets, *rpoB* and *IS6110*,
132 enhances sensitivity and aids discrimination between high and low mycobacterial loads,
133 characterized by double and single positive results, respectively. [13] The ddPCR method applied for
134 HIV-1 quantification was previously developed for use in blood-derived cells[19], *RPP30* was
135 included to quantify and normalise for total human cell count variations across spine biopsy
136 sampling and validating the efficiency of DNA extraction and amplification of MTBC and HIV-1
137 DNA. Information about ddPCR assay set-up, accuracy and calculation of limit of detection of
138 MTBC DNA ddPCR assay and representative ddPCR amplification plots for samples and no
139 template controls are detailed in Supplemental Methods.

140 All pathogen ddPCR data are presented as either total copies/biopsy, or biopsy segment, and gene
141 copy number per million human cells (copies/million cells), unless otherwise specified. Human
142 cell number was calculated estimating two copies of *RPP30* DNA represents one human nucleated
143 cell (see Supplemental Methods). Normalising to cell number allowed pathogen abundance
144 comparison across varying sample types/sizes . *RPP30* copies/µg were compared between biopsy
145 sample types for assessment of tissue cellularity and the relationship to pathogen abundance. For

146 each sample, MTBC and HIV-1 ddPCR results were considered positive if DNA of either gene
147 was detectable above background signal (i.e.: *rpoB* or *IS6110* and *gag* or *pol*, respectively).

148 **Statistics**

149 Descriptive statistics included median values and interquartile range (IQR) for continuous
150 variables and absolute number (n) and frequency (%) for categorical variables. To assess
151 significant differences between groups, Fisher's exact or Kruskal–Wallis tests and Wilcoxon rank
152 sum tests were used for categorical and continuous variables, respectively. A p-value of <0.05 was
153 considered statistically significant. Statistical analyses were conducted using GraphPad Prism
154 Version 9.3.1. For the duplex *rpoB*/IS*6110* and *gag/pol* assays, the categorical variable was the
155 proportion of patients in whom DNA of either gene was detected, and the continuous variable was
156 the number of copies of *rpoB* and IS*6110*/million cells. Sample size was calculated for the original
157 study [24] and samples used in this study represent a convivence sample, such that a formal power
158 calculation was not performed.

159 **Role of the funding source**

160 The funding sources were not involved in the study design nor the execution of the study.

161

162 **RESULTS**

163 **Participant characteristics and total DNA samples for ddPCR derived from spinal biopsies**

164 Of the 31 patients enrolled into the parent study, 25 had sufficient additional tissues collected for
165 the ddPCR sub-study, 10 diagnosed *culture-confirmed STB*, 6 *Xpert Ultra-confirmed STB*, and 9
166 were diagnosed *Not STB* (Figure 1). Patient demographic, clinical and diagnostic characteristics
167 are presented in Table 1 and Supplemental Tables S1-2. Half (8/16) of the patients with confirmed
168 STB, and a third (3/9) of those diagnosed *Not* STB, were males. Those with confirmed SPTB were
169 significantly younger than those without (median age: 40 years *culture-confirmed STB*, 42 years
170 *Xpert-confirmed STB*, 53 years *Not STB*, p=0.02). Of the 25 patients, thirteen (52%) were also
171 PLWH (100% ART established), with no difference in HIV status by TB diagnostic group
172 (p=0.22). Despite all 13 PLWH reporting ART adherence, seven (54%) had detectable peripheral
173 VLs (median copies/ml: 446 (IQR: 294-676)), and 4/13 (31%) were virally suppressed (VL data
174 unavailable for 2). Seventeen (68%) patients underwent open surgery for mechanical stabilization,
175 from which a large tissue biopsy specimen was collected, whilst eight (32%) underwent
176 percutaneous CT-guided biopsy, from which a single core biopsy specimen was collected.

177 **Higher human nucleated cell content in open vs. CT-guided spinal biopsies**

178 From the 25 patients, a total of 93 DNA samples were assayed: open biopsies were portioned into
179 five individual segments/patient (n=17 patients, 85 DNA samples) and CT-guided biopsy were
180 analysed as one sample/patient (n=8 patients, 8 DNA samples) (Table 1, Supplemental Figure S1).
181 Open biopsy samples were variable in tissue size and constitution with diseased hard and soft bone,
182 and other types of diseased tissue (hereafter referred to as 'other') retrieved (Supplemental Table
183 S2). Images of each biopsy are presented in Supplemental Figures S2 and S3. Open biopsy samples

184 had approximately 100-fold higher total DNA recovered and total human nucleated cells
185 (cellularity quantified as two *RRP30* copies/cell), compared to CT-guided biopsies ($p<0.0001$);
186 median total DNA was 149.5 µg (IQR: 38.1 - 217.6 µg) *vs.* 1.865 µg (IQR: 0.69-2.49 µg) and
187 median total cells was 9.94×10^6 (IQR: 4.0×10^6 - 2.5×10^7) *vs.* 8.73×10^4 (IQR: 4.1×10^4 - 2.12
188 $\times 10^5$), respectively. There was no significant difference in the amount of DNA recovered or human
189 cell content between different open biopsy tissue types (Supplemental Figure S4A-D). There was
190 also no significant difference in total cellularity between biopsies from confirmed STB and Not
191 STB patients for either open biopsies ($p=0.1088$) or CT-guided biopsies ($p=0.6429$) (Supplemental
192 Figure S4E) nor by patient HIV-1 status ($p=0.6885$) (Supplemental Figure S4F).

193 **Detection and quantification of MTBC *rpoB* and IS*6110* in total DNA derived from spinal**
194 **biopsy tissues**

195 Assay validation experiments determined both *rpoB* and *IS6110* DNA targets were readily
196 detectable down to 10 fg purified *Mtb* H37Rv DNA (≈2 bacilli equivalent) with LODs determined
197 as 2.29 gene copies/20µl reaction for single-copy *rpoB* and 9.67 copies/20µl reaction for multi-
198 copy *IS6110* (Supplemental Figures S5-S6). In total, 87/93 (94%) biopsy segments produced valid
199 MTBC ddPCR data (>10,000 droplets) (Supplemental Table S2). Mean droplet counts from biopsy
200 tissue reactions with >10,000 droplets measured and mean total volume of droplets/reaction are
201 presented in Supplemental Table S3. 1 µg of total DNA was recovered for MTBC ddPCR reactions
202 for 62/93 (67%) samples. In contrast, 31 (33%) samples (from 17 patients) had low total extracted
203 DNA/segment, resulting in less than 1µg of total DNA added per MTBC ddPCR reaction
204 (minimum added was 46 ng). The minimum amount of DNA loaded/reaction, for which a positive
205 MTBC DNA signal was detected >LOD (*rpoB* or *IS6110*), was 90 ng.

206 Twenty-nine of 87 (34%) biopsy segments with valid data had detectable levels of both *rpoB* and
207 *IS6110*, 16 (18%) segments had only *rpoB* (15) or *IS6110* (1) detected and 42/87 (48%) had
208 undetectable levels of both *rpoB* and *IS6110* (Supplemental Table S4). The higher detection of
209 *rpoB* single positives may be explained by the brighter fluorophore used for this probe. MTBC
210 DNA was detected in 29/39 (74%) segments from *Xpert Ultra-confirmed* and 11/14 (79%)
211 segments from *culture-confirmed* STB patients. Five (15%) of 34 *Not STB* segments had detectable
212 *rpoB* or *IS6110*, of which 2/34 (6%) tissue segments (from two separate patients) were double
213 positive for *rpoB* and *IS6110* (Figure 2A). These five samples came from four patients, all of whom
214 had a previous treated PTB episode, one of whom also had previous treated lymph node TB
215 episode (Supplemental Tables S1-S2). Representative ddPCR amplification plots for samples and
216 no template controls are shown in Supplemental Figures S7-9.

217 For open biopsy tissues, MTBC DNA double positive samples (*rpoB+IS6110+*) were mostly
218 found in segments with >10µg total DNA extracted (Figure 2A). Both STB diagnostic groups had
219 significantly higher *rpoB* and *IS6110* copies/million cells detected than the *Not STB* group
220 ($p \leq 0.0002$) (Figure 2B). For *culture-confirmed* patients, genes detected ranged from 10-6,558
221 copies/million cells for *rpoB* and 55-119,698 copies/million cells for *IS6110*. For *Xpert Ultra-*
222 *confirmed* patients, *rpoB* ranged from 86-389 copies/million cells and *IS6110* ranged from 72-
223 4,045 copies/million cells. For the four *Not STB* patients with detectable MTBC DNA, *rpoB* ranged
224 from 16-61 copies/million cells and *IS6110* from 115-154 copies/million cells (Figure 2B).
225 Analysing samples combined from all patients, *IS6110* and *rpoB* copies/million cells were
226 positively correlated ($r=0.814$, $p<0.0001$, Figure 2C). However, when separating by STB category,
227 correlations remained significant for *culture-confirmed* patients ($r=0.8265$, $p<0.0001$) and *Not STB*
228 patients ($r=0.642$, $p<0.0001$), but not *Xpert Ultra-confirmed* patients ($r=0.1264$, $p=0.6637$). This

229 may be reflective of more *Xpert Ultra-confirmed* patients initiated on TB therapy before biopsy
230 (Table 1), such that more degraded DNA from dead bacteria was detected.

231 As Xpert Ultra and TB culture testing is based on total biopsy sample input, and not on a segment
232 or several segments of a biopsy, we next combined results from the multiple segments obtained
233 from each biopsy. Total gene copies/biopsy ranged from 8-59,144 for *rpoB* and 30-1,001,775 for
234 *IS6110* (Figure 3A) and the total gene copies for the two genes were positively correlated
235 ($r=0.8628$, $p<0.0001$, Figure 3B). There was a significant difference in total gene copies/biopsy
236 for both *rpoB* and *IS6110* between those diagnosed as *Not STB* with *culture-confirmed* patients,
237 but not *Xpert Ultra-confirmed* patients (Figure 3C-D). MTBC DNA (*rpoB* or *IS6110*) was
238 detected in at least one biopsy segment from 19 (76%) of 25 suspected STB patients (Supplemental
239 Table S2 and S4). Stratification by STB diagnostic grouping revealed MTBC DNA was detected
240 >LOD in biopsy tissue from all *culture-confirmed* patients (10/10, 100%), 5/6 (83%) *Xpert Ultra-*
241 *confirmed* patients and 4/9 (44%) *Not STB* patients (Supplemental Table S2). As noted above, the
242 four positive *Not STB* patients had previous TB. Two of these four patients subsequently died, both
243 were *rpoB* DNA positive and one was *rpoB* and *IS6110* double positive (Supplemental Table S1,
244 Figure 3C-D).

245 **HIV-1 DNA is detectable in spinal biopsy tissue from PLWH, irrespective of STB diagnosis**
246 **and peripheral viral load**

247 Next, we investigated the ability of ddPCR to detect HIV-1 DNA in spinal biopsy tissues from the
248 13 PLWH, finding HIV-1 DNA (*pol* and/or *gag*) was detectable all 13 biopsies (Supplemental
249 Table S6). Thirty-four of 37 (92%) tissue segments had detectable HIV-1 DNA, of which 22/37
250 (60%) were positive for both *pol* and *gag,* 10/37 (27%) were positive for *gag* only, and 2/37 (5%)

251 were positive for *pol* only. In patients who underwent open biopsy, HIV-1 DNA (*gag* or *pol*) was
252 detected in all 5 segments from 4/7 (57%) (Supplemental Table S2, Figure 4A). Of the three
253 patients with HIV-1 DNA detected in less than 5 biopsy segments, two had a lower than detectable
254 (LDL) blood VL, and one had VL of 60 copies/ml. In patients who underwent percutaneous CT-
255 guided biopsies, 4/6 (67%) were positive for both *pol* and *gag,* 1/6 (17%) was positive for *gag*
256 only, and 1/6 (17%) positive for *pol* only, with two having LDL blood VL (Supplemental Table
257 S2). When results from PLWH were stratified by STB diagnostic group, HIV-1 DNA was detected
258 in 20/22 (91%) segments from *culture-confirmed STB*, 4/4 (100%) *Xpert Ultra-confirmed* (all CT-
259 guided), and 10/11 (91%) segments from those diagnosed *Not STB* (Supplementary Table S2).
260 Similar to the results for MTBC DNA, double positive segments (Figure 4A, *pol*+*gag*+, green
261 data points) were mostly those with >10µg total DNA extracted, reflecting high tissue cellularity.

262 Overall, HIV-1 *pol* and *gag* copies detected varied at both the patient and sample-type level (Figure
263 4A). Median detected *pol* copies/million cells were 97 (IQR: 39 - 305) and for *gag* were 254 (IQR:
264 75 -519) and *gag* levels were significantly higher than *pol* levels (p=0.0051) (Figure 4B). However,
265 *pol* and *gag* copy numbers/million cells were positively correlated across all biopsy segments
266 (r=0.33, p=0.04) (Figure 4C). Furthermore, restricting the analysis to HIV-1 *pol* and *gag* double
267 positive segments (potentially representing a higher proportion of intact genomes relative to single
268 positive segments, although not directly measurable by the current assay), the positive correlation
269 improved (r=0.7698, p<0.0001).

270 Analysing the relationship between blood and tissue viral abundance, there was also a strong
271 positive correlation between HIV-1 blood VL and the maximum *pol* copies/million cells detected
272 across the biopsy segments tested for each patient (r=0.9072, p=0.0003, Figure 4D). However,
273 there was no significant correlation between maximum detected copies of *gag*/million cells and

274 patient blood VL (r=0.09305, p=0.7856, Figure 4E). This may be due to more *gag* single positive
275 segments, indicative of defective virus, with *gag* being closer to the 5' end of the HIV-1 genome,
276 and/or greater sensitivity of the *gag* ddPCR reaction. HIV-1 DNA, *pol* or *gag* DNA, was detected
277 in all four HIV-positive patients with LDL VL (2 CT-guided biopsies and 2 open surgeries). Of
278 these, three patients had double positive detection of both *pol* and *gag* in one of their biopsy
279 segments (Figure 4A).

280 **MTBC and HIV-1 abundance are increased in spinal tissue segments where both pathogens**
281 **are detected**

282 Analysing the impact of HIV-1 co-infection on overall ddPCR MTBC DNA detection, we found
283 no significant difference by HIV-1 status, with *IS6110* and/or *rpoB* detected in biopsy tissues from
284 11/13 (85%) PLWH and from 8/12 (67%) HIV-1 uninfected patients (p=0.378) (Supplemental
285 Table S7). In line with our previous findings for *Mtb* abundance measured by culture and Xpert
286 Ultra[24], there was also no difference by HIV-1 status in MTBC *rpoB* or *IS6110* total DNA copies
287 detected per biopsy (Figure 5A). However, when analysing results normalised to biopsy segment
288 cellularity, *rpoB* and *IS6110* copies/million cells were significantly higher in biopsies from PLWH
289 (Figure 5B-C, p=0.0096 and p=0.0118, respectively).

290 To further investigate the interaction between HIV-1 and *Mtb* at the site of disease we next
291 investigated the presence and abundance of both pathogens in each biopsy segment. Valid ddPCR
292 data for both MTBC and HIV-1 DNA detection were obtained for 35/41 biopsy segments from 13
293 PLWH (the remaining 6 tissue segments had <10,000 droplets for either MTBC or HIV-1
294 detection). Eleven of the 13 (92%) patients had co-detection of MTBC and HIV-1 DNA in at least
295 one of their open biopsy tissue segments (n=7) or in the whole percutaneous biopsy (n=4) (Figure

296 5D). 20/35 (57%) segments had both MTBC and HIV-1 DNA detected (*rpoB* and/or *IS6110* AND
297 *pol* and/or *gag*). Of these 16/20 (80%) were double positive for MTBC genes (*rpoB+/IS6110+),*
298 the remaining four were *rpoB* positive only, and 16/20 (80%) samples were double positive for
299 HIV-1 genes (*pol+/gag+),* with two samples single positive for *pol* and two for *gag*. In total, 14/20
300 (70%) samples were double positive for both MTBC *rpoB+/IS6110+* and HIV-1 *pol+/gag+*.

301 Within individual biopsy segments, single copy MTBC gene *rpoB* copies/million cells were also
302 positively correlated with detected HIV-1 *pol* DNA copies/million cells (r=0.3963, p=0.0003) in
303 the same segment, whilst there was no significant correlation between MTBC *rpoB* and HIV-1
304 *gag* copies/million cells (p=0.3595) (Figure 5E-F). As we found the maximum biopsy segment
305 HIV-1 *pol* DNA copies/million cells, was strongly correlated with blood VL, we also analysed the
306 relationship of VL to total biopsy MTBC *rpoB* copies and maximum biopsy segment *rpoB*
307 copies/million cells. Both were not significantly correlated with blood VL, indicating *Mtb*
308 abundance at STB biopsy sites is positively correlated with local HIV-1 abundance and not
309 peripheral VL (Figure 5G-H). Finally, we tested whether the abundance of HIV-1 DNA in spinal
310 tissue segments from PLWH on ART is increased in tissues where MTBC DNA was detected. On
311 a tissue segment basis*, pol* gene copies/million cells were significantly higher in samples where
312 MTBC DNA was detected (p=0.0110), whilst there was no significant difference for *gag*
313 copies/million cells by MTBC DNA presence (p=0.6002) (Figure 5I-J).

314 **DISCUSSION**

315 Here we report the findings of the first study, to our knowledge, to test for MTBC-complex DNA
316 and the presence of HIV-1 DNA in spinal biopsy tissue from patients investigated for STB, living
317 in a setting with a high incidence of both TB and HIV-1 infection. A high proportion of our patients
318 were PLWH (52%) consistent with a previous local study of STB reporting a HIV-1-infectivity
319 rate of 50%.[25] The ddPCR assay successfully detected and quantified MTBC DNA in biopsy
320 tissues, confirming MTBC detection in 94% of patients with positive Xpert Ultra results. The
321 ddPCR assay also detected MTBC DNA in biopsies from four patients in which *Mtb* could not be
322 detected by culture or Xpert Ultra, all of whom had a previous TB diagnosis. Furthermore HIV-1
323 DNA was successfully detected in the spinal tissues of all PLWH, all of whom were established
324 on ART, including four who were peripherally virally suppressed, with HIV-1 *pol* copies/million
325 cells correlating with blood VL. We found MTBC *rpoB* and *IS6110* copies/million cells were
326 significantly higher in spinal tissue segments from PLWH. Moreover, HIV-1 *pol* copies/million
327 cells were significantly higher in spinal tissue segments in which MTBC DNA was co-detected
328 and positively correlated with co-detected MTBC *rpoB* copies/million cells. Finally, we
329 determined that tissue *Mtb* abundance quantified by *rpoB* copies/million cells positively correlated
330 with tissue HIV-1 *pol* copies and not blood VL, suggestive of a localised relationship between
331 these co-infecting pathogens.

332

333 We provide evidence for the sensitive detection of MTBC-specific DNA, using a previously
334 described assay for assessing the LOD for each gene[16, 26], within spinal biopsy tissues of 19 of 25
335 suspected STB patients. We expect that *Mtb* will be predominantly intracellular, but may also be
336 extracellular, and thus comparing the abundance of *Mtb* relative to human cellular abundance, may

337 inform the cellularity of the tissue within which high amounts of *Mtb* DNA is found. We also
338 postulated that with *Mtb* infection, tissues at the site of disease may be more abundant with
339 recruited and infiltrated cells, however, neither the abundance of *Mtb* infection in the spine nor the
340 abundance of HIV-1 co-infection was associated with the cellularity of the biopsy obtained
341 although there were trends observed. However normalising *Mtb* abundance to biopsy human cell
342 numbers, identified a significant increase in *Mtb* abundance at the site of STB in PLWH, that was
343 not previously found when merely comparing *Mtb* abundance based on total biopsy culture or
344 Xpert.[24]
345 The high sensitivity of ddPCR, also enabled low-level detection of MTBC DNA in four patients
346 who were clinically diagnosed STB negative based on culture and Xpert Ultra, all of whom had
347 previous PTB and two were PLWH. Notably, 68% of the patients with *Mtb* DNA detected in their
348 biopsies by ddPCR had a previous TB episode. *Mtb* may have seeded in the spine via a
349 haematogenous route following pulmonary or lymph node disease. In the case of the four patients
350 diagnosed *Not STB,* the detected MTBC DNA may have arisen from this previous haematogenous
351 seeding of *Mtb* in the spine that was no longer viable so culture negative, or it represents a
352 misdiagnosis by culture and Xpert Ultra of a new TB episode detectable by ddPCR. It cannot be
353 ruled out that the positive result was due to cross-contamination or non-specific amplification,
354 however all 14 biopsy segments from those diagnosed *Not STB* with no previous TB were *rpoB*
355 and *IS6110* negative as were no template controls.
356
357 Comparing our level of MTBC DNA detection to that in other TB studies, our calculated mean of
358 367 *IS6110* copies/20µl is within the range of 10 - 1000 *IS6110* copies/20µl reported by Belay *et*
359 *al.*[16] Two other MTBC DNA ddPCR studies reported ~10 copies of *IS6110*/20µl in plasma from

360 EPTB patients[27] and a contrasting high equivalent average of 3686 copies *IS6110*/20µl from whole
361 blood-derived DNA samples from patients with PTB/EPTB (n=12 patients with bone TB).[28] The
362 insertion sequence (IS) has been used successfully for the diagnosis of *Mtb,* however, some *Mtb*
363 clinical strains are IS6110-negative, leading to false negative results.[29] Use of double-gene target
364 assays, including *IS6110* and other MTBC specific genes, *IS1081* and *rpoB*[15, 16], in paucibacillary
365 samples, enhances sensitivity and aids discrimination between high and low mycobacterial loads,
366 characterized by double and single positive results, respectively.[13]
367
368 *Gag* and *pol* DNA was successfully detected in biopsy tissues of all PLWH in our study. To our
369 knowledge, this is the first study to use ddPCR to detect and quantify HIV-1 at the site of STB
370 disease. HIV-1 DNA was detected in biopsies from patients with no detectable viral loads in the
371 blood, potentially indicating tissue-specific presence and persistence. It is well known that HIV-1
372 integrates into the host genome as a provirus and can establish latency shortly after infection.[30] As
373 ART only inhibits actively replicating virus, it cannot eliminate the virus from latently infected
374 cells, which persist through mechanisms such as homeostatic proliferation [31] and represent a source
375 of viral rebound, if treatment is interrupted.[32] In a recent review[22], we presented a rationale for
376 how the inflammatory state during active *Mtb* infection has the potential to both enhance viral
377 replication, by driving transcription of HIV-1 genes from the HIV long terminal repeat promoter
378 region, and to create an expanded cellular niche that is susceptible to HIV-1 infection. This may
379 contribute to detectable viral loads[22], albeit at low levels as ART adherence should prevent ongoing
380 rounds of viral replication and rebound. While multiple factors can influence suppression of HIV
381 VL, based on findings in our study, we hypothesize that HIV-1 tissue reservoirs at the site of STB
382 inflammation may contribute to HIV-1 transcriptional activation and increased detection of

383 circulating HIV-1 in these patients. However, since the HIV reservoir is composed of
384 predominantly replication defective virus[33], only a limited proportion of latently infected cells can
385 give rise to replication-competent viruses. Thus, more may be at play in the context of co-infection,
386 driving ongoing HIV viral replication. Identifying tissue-based and specific cellular reservoirs of
387 HIV-1 in patients on ART is critical to finding a cure for the virus. Recently, Chaillon *et al.*,[34]
388 analysed HIV-1 reservoirs in both the blood, prior to death, and from various anatomical tissue
389 sites, during post-mortems, of PLWH using ddPCR and showed evidence of the persistence of
390 HIV in 27 deep anatomical sites including the colon, lymph nodes, and spleen. A prior study
391 examined HIV-1 persistence in ART-treated individuals with undetectable plasma HIV-1 RNA
392 levels and found PCR evidence of HIV-1 DNA in freshly isolated CD34+ bone marrow cells in
393 44% of patients.[35] In addition, the detection of HIV proviral DNA (median: 62 copies/million cells)
394 in bone marrow, using Realtime quantitative PCR (qPCR), was reported for Zambian individuals
395 suppressed on ART in the first study to characterize HIV persistence in different anatomical sites[36].
396 The Last Gift study analysed post-mortem tissue samples for the presence of HIV deep tissue
397 reservoirs, and utilised ddPCR to measure HIV proviral copy number in the spinal cord and
398 reported unexpectedly high levels of HIV at this site.[37] These reservoirs could be targeted for
399 therapy either through cell-based drug delivery or by taking advantage of their close interaction
400 with CD4+ cells, which are known to be a target of HIV-1 infection.[38]
401
402 Overall, significant relationships were highlighted using the *pol* gene over the *gag* gene in samples
403 where MTBC DNA was also detected and a strong positive correlation between *pol* and *rpoB*
404 copies/million cells. Overall *gag* copy numbers appeared to be higher than *pol*. We cannot rule out
405 that either the *pol* primer/probe set was less sensitive to provirus detection or that the *gag*

406 primer/probe set may have produced off-target, background amplification signal, resulting in the
407 discrepancies. As stated, the vast majority of HIV-1 proviral genomes are defective (either
408 hypermutated or harbouring large internal deletions)[33], and copy numbers of these two genes are
409 not expected to be highly correlated. Most HIV-1 studies have focussed on whole blood and bone
410 marrow aspirates for the detection of HIV-1 DNA. The Intact Proviral DNA Assay (IPDA) is a
411 potential future improvement to our method, as it permits discrimination of defective proviral
412 populations through amplification of targets that have an increased statistical likelihood of being
413 present together only in intact genomes.[18] Since viral reactivation and rebound would originate
414 from the pool of cells harbouring intact proviral genomes, this could provide an opportunity to
415 quantify the number of cells that can produce HIV in tissues that are also positive for *Mtb*. In
416 future, isolation of specific cell populations from spinal biopsy tissues and flow cytometry or single
417 cell omics in combination with ddPCR methods that distinguish intact viral genomes from those
418 that are defective, as mentioned above, will aid in characterization of HIV-1 in these populations
419 and specific cellular reservoirs. This will ultimately guide the improvement of TB and HIV-1 cure
420 strategies that are specifically tailored to treat this potentially deadly syndemic.
421
422 The small sample size is a limitation of our study. This was due to the impact of the COVID-19
423 pandemic and the change in hospital seeking nature of our patients during enrolment period. In
424 addition, the study was conducted at a single site. The study did not have a true TB negative control
425 group, given the high rates of previous pulmonary TB in the *Not STB* group, confounding whether
426 detection of MTBC DNA in the spine of those diagnosed as *Not STB* was due to current mis-
427 diagnosis or migration of the previous infection that was no longer viable to the new clinical
428 presentation. Future work should include the assessment of MTBC 16S mRNA as a

429 complementary analysis to the detection of *rpoB* and *IS6110* DNA using ddPCR to inform
430 potential viability of *Mtb*. More parallel studies using larger sample sizes, targeting more
431 sequences, or involving different stages of disease, are needed to further clarify the diagnostic
432 value of ddPCR for STB. ddPCR is not yet widely available, and widespread implementation has
433 been hindered by the relatively high current cost per ddPCR reaction, compared with standard
434 qPCR and more complex infrastructure and specialized personnel requirements.[39, 40] However,
435 recent innovations in chip-based vs droplet generation systems will likely overcome these factors.
436 Future work should also compare the detection of MTBC and HIV-1 DNA in the peripheral blood,
437 with the site of disease and how these may change with treatment. This would only be possible in
438 patients who have repeated biopsies after they have been initiated on anti-tuberculous therapy for
439 a certain level of time. Finally, we did not measure HIV RNA or proteins in tissue biopsies. Such
440 assays could determine whether local replication of HIV is induced at sites of TB co-infection to
441 confirm the TB inflammatory microenvironment facilitates HIV-1 reservoir persistence and
442 activation in those ART established and peripherally suppressed.

443 In conclusion, rapid diagnosis of TB is crucial for patient treatment and outcome and for infection
444 control. We report ddPCR can provide simple and rapid diagnosis of *Mtb* infection, including in
445 the context of HIV-1 infection, and may have superior sensitivity over Xpert Ultra, detecting low
446 levels of DNA in 4 patients not diagnosed with STB by conventional molecular microbiological
447 testing. We also report the co-localisation of both pathogens facilitates expansion of the other at
448 the site of TB disease and this needs to be considered with detection methods and tailored treatment
449 strategies that ensure penetrance into anatomical sites such as the spine. The contribution of the
450 TB microenvironment as both a reservoir and site of HIV reservoir activation requires further
451 investigation.

452 **DATA SHARING**

453 Deidentified data from this study will be made available upon request with investigator support,
454 after approval of a proposal, and with a signed data access agreement. For data access, please
455 contact the corresponding author.

456 **ACKNOWLEDGMENTS.**

457 Nomsa Yekiso, Nosipho Mncwabe, Dr Qonita Hartley, Dr Chad Centner, Ms Nawaal Adikary and
458 Zeenat Hoosen, orthopaedic surgical teams and our patients for helping, participating and
459 contributing to global evidence. The following reagent was obtained through the NIH HIV Reagent
460 Program, Division of AIDS, NIAID, NIH: HIV-1 Lymphadenopathy-Associated Virus (LAV)-
461 Infected 8E5 Cells, ARP-95, contributed by Dr Thomas Folks.

462 **DECLARATION OF INTERESTS**

463 The authors have declared that no conflict of interest exists.

464 **CONTRIBUTORS**

465 RW collected tissues, performed assays, analysed data and drafted the manuscript. ACK, MRA,
466 MH, and ARM contributed to study design, supported data collection and analysis, and edited the
467 manuscript. RND and ML aided study design, input and sample collection. For the purposes of
468 open access, the authors have applied a CC-BY public copyright to any author-accepted
469 manuscript arising from this submission.

470

471

472 **REFERENCES**

473 1. Perkins MD, Cunningham J. Facing the crisis: improving the diagnosis of tuberculosis in
474 the HIV era. The Journal of infectious diseases. 2007;196(Supplement_1):S15-S27.

475 2. Davies P, Pai M. The diagnosis and misdiagnosis of tuberculosis [State of the art series.
476 Tuberculosis. Edited by ID Rusen. Number 1 in the series]. The International Journal of
477 Tuberculosis Lung Disease. 2008;12(11):1226-34.

478 3. Adeyemo S, Sangotola A, Korosteleva O. Modeling transmission dynamics of
479 tuberculosis–HIV co-infection in South Africa. Epidemiologia. 2023;4(4):408-19.

480 4. Rajasekaran S, Soundararajan DCR, Shetty AP, Kanna RM. Spinal Tuberculosis: Current
481 Concepts. Global Spine Journal. 2018;8(4 Suppl):96s-108s.

482 5. Govender S, Annamalai K, Kumar K, Govender U. Spinal tuberculosis in HIV positive and
483 negative patients: immunological response and clinical outcome. International orthopaedics.
484 2000;24:163-6.

485 6. Dunn R, Husien MB. Spinal tuberculosis: review of current management. The bone & joint
486 journal. 2018;100(4):425-31.

487 7. Dunn R. The medical management of spinal tuberculosis. SA Orthopaedic Journal.
488 2010;9:37-41.

489 8. Held M, Laubscher M, Dix-Peek S, Zar H, Dunn R, editors. Accuracy of GeneXpert PCR
490 Testing in Osteoarticular TB. Orthopaedic Proceedings; 2014: The British Editorial Society of
491 Bone & Joint Surgery.

492 9. Held M, Laubscher M, Zar HJ, Dunn RN. GeneXpert polymerase chain reaction for spinal
493 tuberculosis: an accurate and rapid diagnostic test. Bone Joint Journal. 2014;96-b(10):1366-9.

494 10. Dunn R, Zondagh I. Spinal tuberculosis: Diagnostic biopsy is mandatory. SAMJ: South
495 African Medical Journal. 2008;98(5):360-2.

496 11. Dunn RN, Ben Husien M. Spinal tuberculosis: review of current management. Bone Joint
497 Journal. 2018;100-b(4):425-31.
498 12. Cao Z, Wu W, Wei H, Gao C, Zhang L, Wu C, et al. Using droplet digital PCR in the
499 detection of Mycobacterium tuberculosis DNA in FFPE samples. International Journal of
500 Infectious Diseases. 2020;99:77-83.
501 13. Antonello M, Scutari R, Lauricella C, Renica S, Motta V, Torri S, et al. Rapid Detection
502 and Quantification of Mycobacterium tuberculosis DNA in paraffinized samples by droplet digital
503 PCR: a preliminary study. Frontiers in microbiology. 2021;12.
504 14. Yang J, Han X, Liu A, Bai X, Xu C, Bao F, et al. Use of Digital Droplet PCR to Detect
505 Mycobacterium tuberculosis DNA in Whole Blood-Derived DNA Samples from Patients with
506 Pulmonary and Extrapulmonary Tuberculosis. Front Cell Infect Microbiol. 2017;7:369.
507 15. Nyaruaba R, Mwaliko C, Kering KK, Wei H. Droplet digital PCR applications in the
508 tuberculosis world. Tuberculosis (Edinb). 2019;117:85-92.
509 16. Belay M, Tulu B, Younis S, Jolliffe DA, Tayachew D, Manwandu H, et al. Detection of
510 Mycobacterium tuberculosis complex DNA in CD34-positive peripheral blood mononuclear cells
511 of asymptomatic tuberculosis contacts: an observational study. The Lancet Microbe. 2021.
512 17. Karris MA, Smith DM. Tissue-specific HIV-1 infection: why it matters. Future virology.
513 2011;6(7):869-82.
514 18. Buchholtz N, Nühn M, de Jong T, Stienstra T, Reddy K, Ndung'u T, et al. Development
515 of a highly sensitive and specific intact proviral DNA assay for HIV-1 subtype B and C. Virology
516 Journal. 2024;21(1):1-11.
517 19. Strain MC, Lada SM, Luong T, Rought SE, Gianella S, Terry VH, et al. Highly precise
518 measurement of HIV DNA by droplet digital PCR. J PloS one. 2013;8(4):e55943.

519 20. Bruner KM, Wang Z, Simonetti FR, Bender AM, Kwon KJ, Sengupta S, et al. A
520 quantitative approach for measuring the reservoir of latent HIV-1 proviruses. Nature.
521 2019;566(7742):120-5.
522 21. Cassidy NA, Fish CS, Levy CN, Roychoudhury P, Reeves DB, Hughes SM, et al. HIV
523 reservoir quantification using cross-subtype multiplex ddPCR. iScience. 2022;25(1).
524 22. Waters R, Ndengane M, Abrahams M-R, Diedrich CR, Wilkinson RJ, Coussens AK. The
525 Mtb-HIV syndemic interaction: why treating M. tuberculosis infection may be crucial for HIV-1
526 eradication. Future virology. 2020;15(02):101-26.
527 23. He X, Eddy JJ, Jacobson KR, Henderson AJ, Agosto LM. Enhanced human
528 immunodeficiency virus-1 replication in CD4+ T cells derived from individuals with latent
529 mycobacterium tuberculosis infection. The Journal of infectious diseases. 2020;222(9):1550-60.
530 24. Waters R, Laubscher M, Dunn RN, Adikary N, Coussens AK, Held M. Higher sensitivity
531 of Xpert MTB/RIF Ultra over Tuberculosis Culture for the diagnosis of spinal tuberculosis with
532 Open or computed tomography–guided biopsies. Open Forum Infectious Diseases. 2024;11(1).
533 25. Mann TN, Davis JH, Walzl G, Beltran CG, Du Toit J, Lamberts RP, et al. Candidate
534 biomarkers to distinguish spinal tuberculosis from mechanical back pain in a tuberculosis endemic
535 setting. Frontiers in Immunology. 2021:4903.
536 26. Armbruster DA, Pry T. Limit of blank, limit of detection and limit of quantitation. The
537 clinical biochemist reviews. 2008;29(Suppl 1):S49.
538 27. Lyu L, Li Z, Pan L, Jia H, Sun Q, Liu Q, et al. Evaluation of digital PCR assay in detection
539 of M. tuberculosis IS6110 and IS1081 in tuberculosis patients plasma. BMC Infectious Diseases.
540 2020;20(1):1-9.

541 28. Yang J, Han X, Liu A, Bai X, Xu C, Bao F, et al. Use of digital droplet PCR to detect
542 Mycobacterium tuberculosis DNA in whole blood-derived DNA samples from patients with
543 pulmonary and extrapulmonary tuberculosis. Frontiers in cellular infection microbiology.
544 2017;7:369.
545 29. Zhou L, Ma C, Xiao T, Li M, Liu H, Zhao X, et al. A new single gene differential biomarker
546 for Mycobacterium tuberculosis complex and non-tuberculosis mycobacteria. Frontiers in
547 microbiology. 2019;10:1887.
548 30. Chavez L, Calvanese V, Verdin E. HIV latency is established directly and early in both
549 resting and activated primary CD4 T cells. PLoS pathogens. 2015;11(6):e1004955.
550 31. Chomont N, El-Far M, Ancuta P, Trautmann L, Procopio FA, Yassine-Diab B, et al. HIV
551 reservoir size and persistence are driven by T cell survival and homeostatic proliferation. Nature
552 medicine. 2009;15(8):893-900.
553 32. Price A, Shearman AD, Hamilton TW, Alvand A, Kendrick B, Bone C-NSTJ, et al. 30-day
554 outcome after orthopaedic surgery in patients assessed as negative for COVID-19 at the time of
555 surgery during the peak of the pandemic. 2020;1(8):474-80.
556 33. Bruner KM, Murray AJ, Pollack RA, Soliman MG, Laskey SB, Capoferri AA, et al.
557 Defective proviruses rapidly accumulate during acute HIV-1 infection. Nature medicine.
558 2016;22(9):1043-9.
559 34. Chaillon A, Gianella S, Dellicour S, Rawlings SA, Schlub TE, De Oliveira MF, et al. HIV
560 persists throughout deep tissues with repopulation from multiple anatomical sources. The Journal
561 of clinical investigation. 2020;130(4):1699-712.

562 35. Carter CC, Onafuwa-Nuga A, McNamara LA, Riddell IV J, Bixby D, Savona MR, et al.
563 HIV-1 infects multipotent progenitor cells causing cell death and establishing latent cellular
564 reservoirs. Nature medicine. 2010;16(4):446-51.
565 36. Liu Z, Julius P, Kang G, West JT, Wood C. Subtype C HIV-1 reservoirs throughout the
566 body in ART-suppressed individuals. JCI insight. 2022;7(20).
567 37. Riggs PK, Chaillon A, Jiang G, Letendre SL, Tang Y, Taylor J, et al. Lessons for
568 Understanding Central Nervous System HIV Reservoirs from the Last Gift Program. J Current
569 HIV/AIDS Reports. 2022:1-14.
570 38. Araínga M, Su H, Poluektova LY, Gorantla S, Gendelman HE. HIV-1 cellular and tissue
571 replication patterns in infected humanized mice. Scientific reports. 2016;6(1):23513.
572 39. Hindson BJ, Ness KD, Masquelier DA, Belgrader P, Heredia NJ, Makarewicz AJ, et al.
573 High-throughput droplet digital PCR system for absolute quantitation of DNA copy number. Anal
574 Chem. 2011;83(22):8604-10.
575 40. Campomenosi P, Gini E, Noonan DM, Poli A, D'Antona P, Rotolo N, et al. A comparison
576 between quantitative PCR and droplet digital PCR technologies for circulating microRNA
577 quantification in human lung cancer. BMC biotechnology. 2016;16(1):1-10.

578

579 **Table 1. Study patient characteristics, stratified by patient diagnostic group.**

	Overall	**TBCUL+GXPU+HIST+** *(Culture confirmed)*	**TBCUL-GXPU+HIST+** *(Xpert Ultra confirmed)*	**TBCUL-GXPU-HIST-** *(Not STB)*
Total Patients	25 (100%)	10 (40%)	6 (24%)	9 (36%)
Age, years	48 (36-53)	40 (29 – 49)	42 (38-44)	53 (49-58)
Male sex	11 (44%)	5 (50%)	3 (50%)	3 (33%)
HIV-1 positive	13 (52%)	6 (60%)	4 (67%)	3 (33%)
Detectable HIV-1 viral load	7/11[A] (64%)	3/5[a] (60%)	2/3[A] (67%)	2/3 (67%)
Viral load	446 (294-791)	372 (292 -391)	1137 and 49959	60 and 676
Previous TB history	14 (56%)	5 (50%)	4 (67%)	5 (56%)
TB therapy initiated before biopsy	9 (28%)	3 (30%)	5 (83%)	1 (11%)
TB culture positive	10 (40%)	10 (100%)	0 (0%)	0 (0%)
Xpert MTB/RIF Ultra +	16 (64%)	10 (100%)	6 (100%)	0 (0%)
Histopathology +	12/19[B] (63%)	7/7 (100%)	5/5 (100%)	0/7 (0%)
AFB +	2/18[C] (11%)	2/8 (25%)	0/5 (0%)	0/5 (0%)
Open biopsy	17 (68%)	8 (80%)	2 (33%)	7 (78%)
CT-guided biopsy	8 (32%)	2 (20%)	4 (67%)	2 (22%)
Total DNA samples	93 (100%)	42 (45%)	14 (15%)	37 (40%)

580 Data are proportion (n) and (%) or median (IQR). [A]n=2 unavailable VL results (1 culture confirmed and 1 Xpert
581 Ultra confirmed); n=4 lower than detectable limit (LDL); [B]No histology report available in n=6 patient (3 culture
582 confirmed, 1 Xpert Ultra confirmed, 2 Not STB); [C]No ZN staining report available in n=7 patients. +: positive; -:
583 negative; AFB: acid fast bacilli; ART, antiretroviral therapy; CT: Computed tomography; CUL culture; GXPU:
584 Xpert MTB/RIF Ultra; HIST: histology; TB: Tuberculosis.

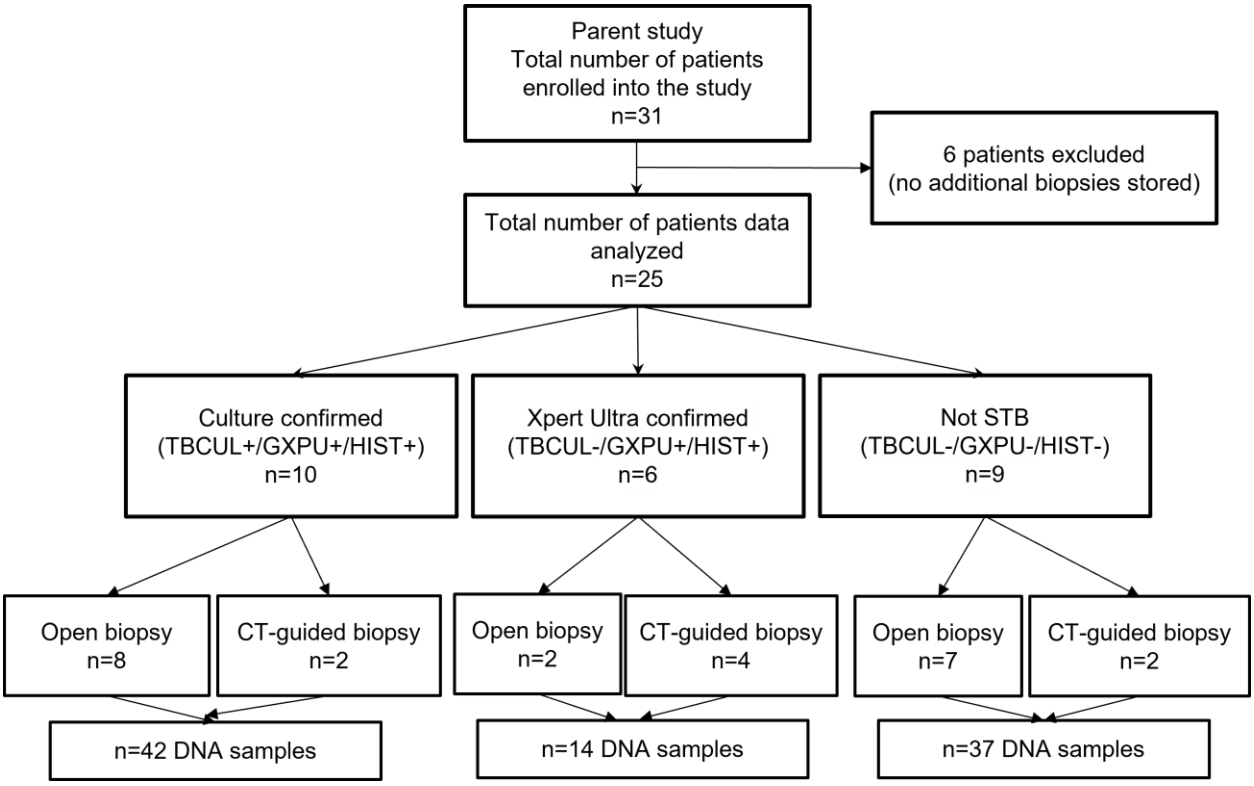

Figure 1. Flow diagram of study patients including diagnostic, surgical, and ddPCR sample categories. *GXPU: Xpert MTB/RIF Ultra; TBCUL: MGIT TB culture; HIST: histology including histopathology and Ziehl-Neelsen stain for acid fast bacilli.*

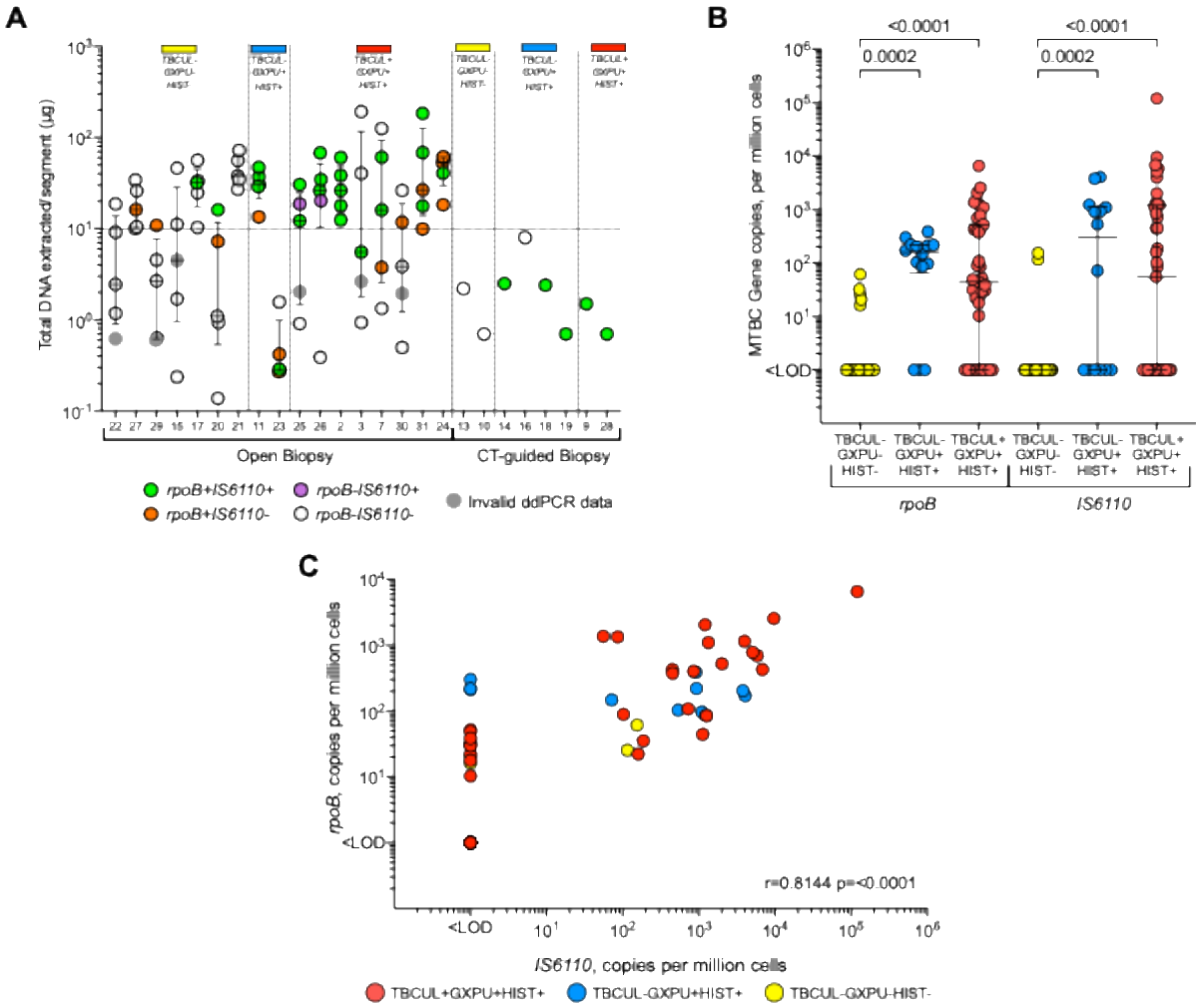

Figure 2. MTBC *rpoB* and *IS6110* copies detected by ddPCR. **A)** MTBC DNA detection in total DNA extracted per segment of open biopsy patients, stratified by STB diagnostic group**.** Individual dots represent total DNA extracted per biopsy segment (n=5 open biopsy, n=1 CT-guided biopsy). Double positives (*rpoB+IS6110+*, green dots; no *rpoB* or *IS6110* detected (*rpoB-IS6110-,* white dots with black border); single positives (*rpoB+IS6110-,* orange dots; single positives (*rpoB-IS6110+,* purple dots). X-axis labelled with patient ID. **B)** Gene copies in biopsy segments, stratified by STB diagnostic grouping**.** *rpoB* and *IS6110* copy numbers per million human cells for n=87 segments with valid ddPCR data. <LOD was 'undetectable'. p-values were calculated using Kruskal-Wallis Test with FDR = 0.1, two-stage step-up (Benjamini, Krieger and Yekutieli). Lines show median values with IQR. **C)** *IS6110* versus *rpoB* copies/million cells for the 87 biopsy segments with valid ddPCR data. X and Y axes are log10. Spearman Correlation coefficients and p values were calculated using Spearman's test. *GXPU: Xpert MTB/RIF Ultra, HIST: Histology, LOD: Limit of detection, TBCUL: MGIT TB culture.*

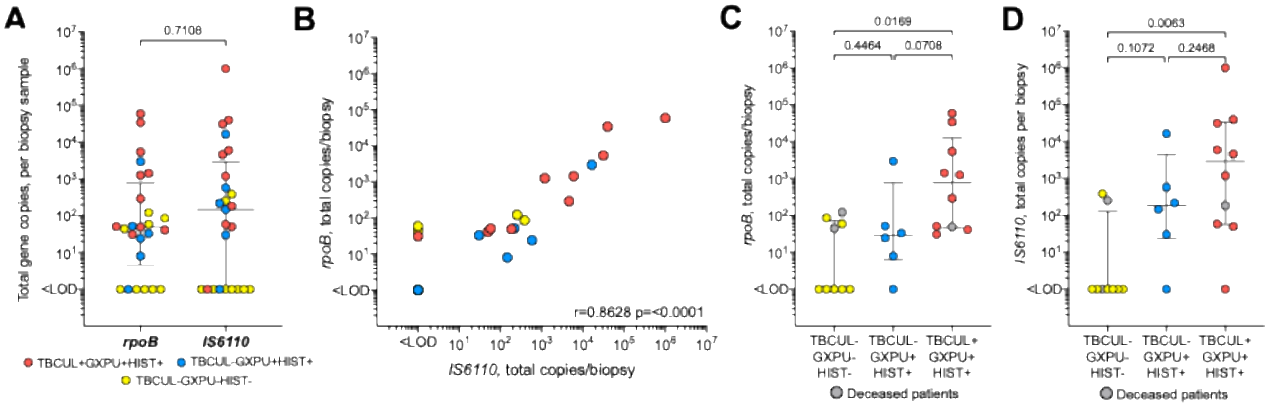

Figure 3. Total MTBC gene copies per biopsy from adult patients investigated for STB, undergoing either percutaneous CT-guided biopsy or open biopsy in theatre. A) Total *rpoB* and *IS6110* copies, per total biopsy, **B**) Spearman's correlation between *IS6110* and *rpoB* total copies per biopsy, **C**) Total *rpoB* and D) *IS6110* copies per biopsy, stratified by STB diagnostic group. Grey dots represent deceased patients who passed away after diagnosis. Data are presented as median and IQR. Individual dots represent entire combined biopsy results for each patient. Kruskal-Wallis test with FDR=0.1 two-stage step-up (Benjamini, Krieger and Yekutieli) was used. *GXPU: Xpert MTB/RIF Ultra, HIST: Histology, LOD: Limit of detection, TBCUL: MGIT TB culture.*

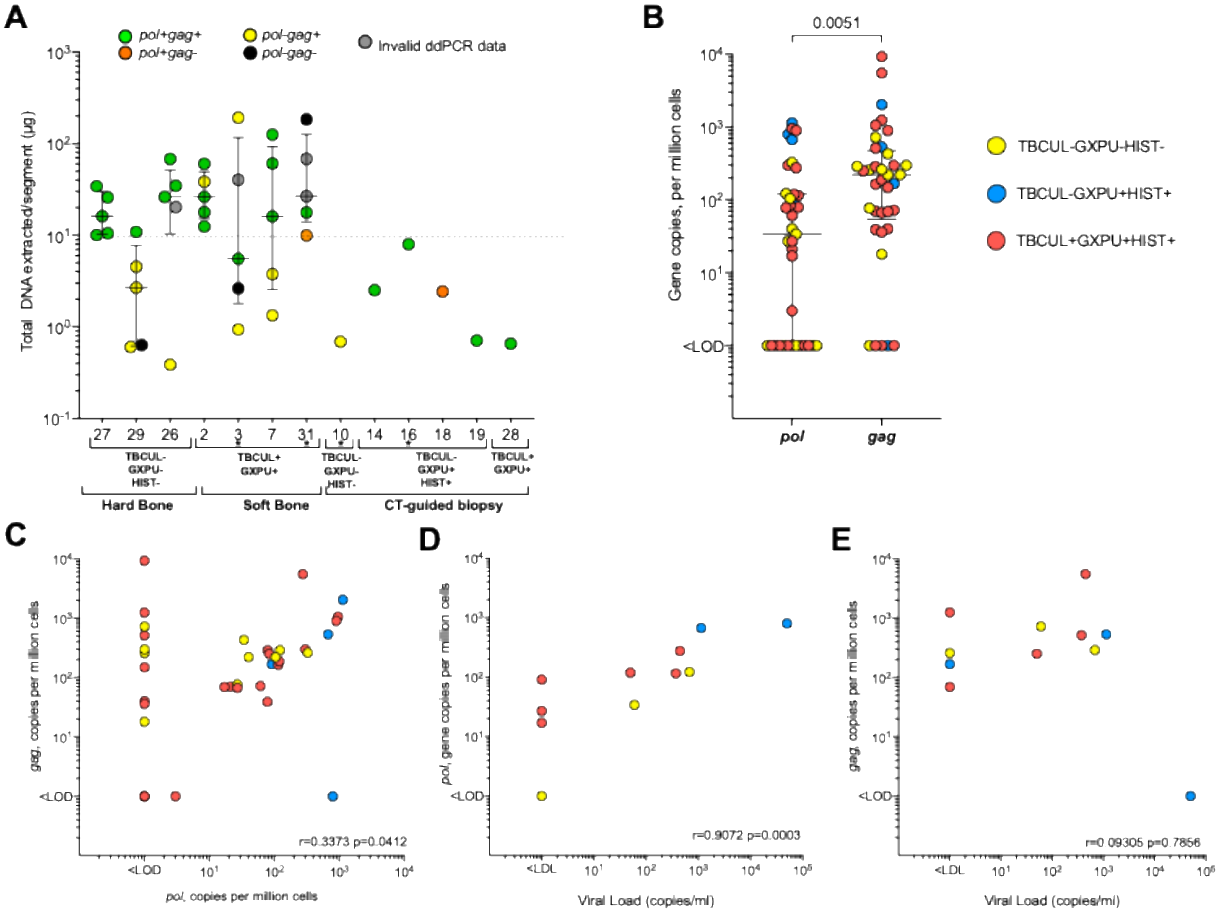

Figure 4. Detection of HIV-1 DNA in spinal biopsy tissue from PLWH and the relationship to viral load. A) HIV-1 DNA detection in total DNA extracted per segment of open biopsy from PLWH, stratified by STB diagnostic group and type of tissue extracted during surgery. Individual dots represent total DNA extracted per five biopsy segments from each patient. X axis is patient study ID. *Pol* and *gag*: HIV-1 genes. Invalid ddPCR: samples with droplet counts <10 000, no detection by software. * on PID indicates patient had blood viral load lower than detectable levels. **B**) Detection and **C**) correlation of HIV-1 *pol* and *gag* gene copies per million cells in DNA from biopsy tissues of adult suspected spinal tuberculosis patients. Correlation between spinal biopsy maximum detected **D**) *pol* and **E**) *gag*, copies per million cells across tested biopsy segments vs. HIV-1 VL in the blood. Correlation coefficients and p-values were calculated with Spearman's test. n=2 patients had unknown viral loads and were excluded from D and E analysis. *GXPU: Xpert MTB/RIF Ultra; HIST: Histology; TBCUL: MGIT TB culture.*

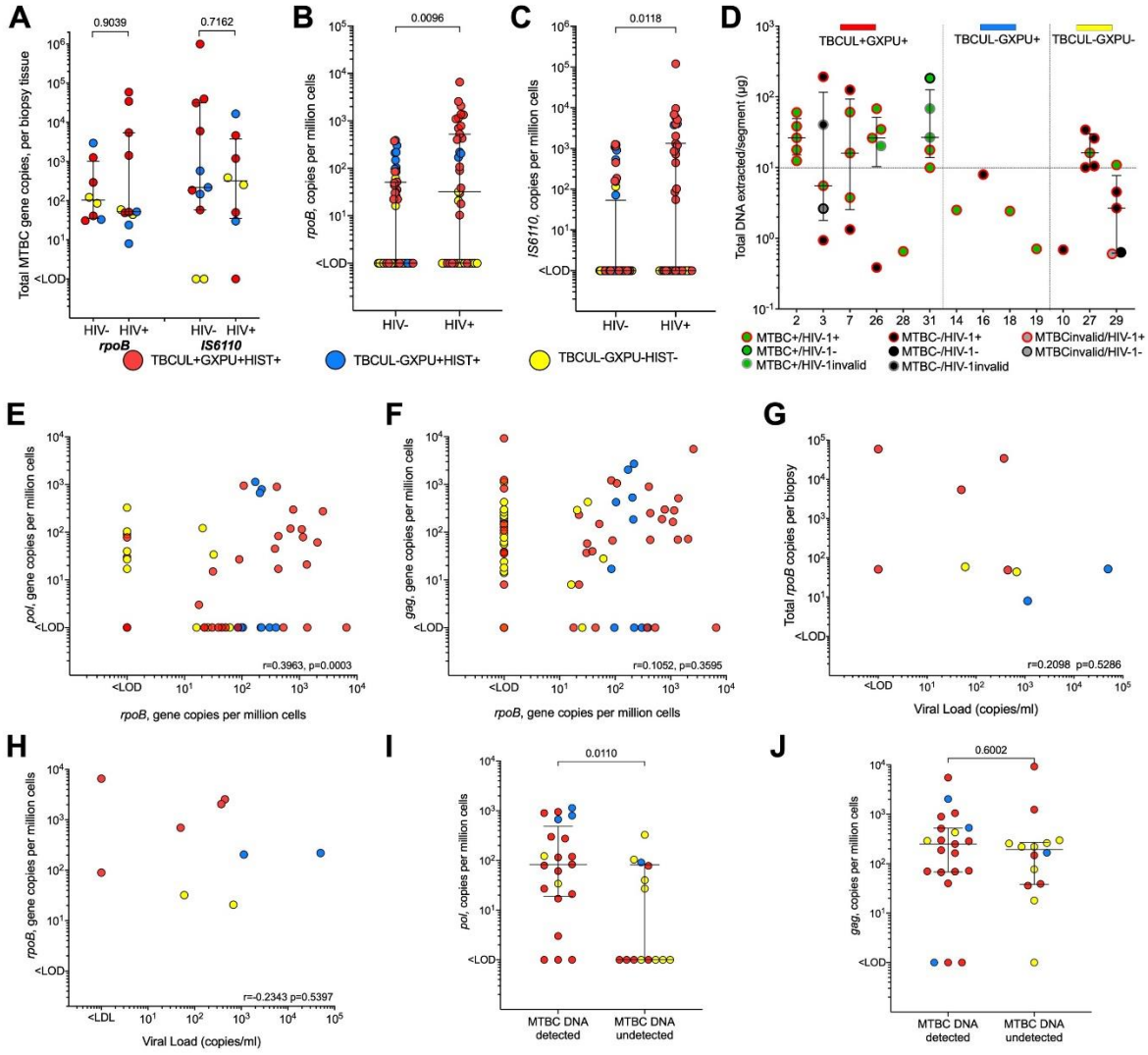

Figure 5. Relationship between MTBC DNA abundance and HIV-1-status, gene copies, and co-detection of MTBC DNA in spinal TB biopsy tissues. A) Total *rpoB* and *IS6110* copies, per total biopsy tissue by HIV status. MTBC *rpoB* (**B**) and *IS6110* (**C**) copy numbers/million cells in DNA from biopsy segments by patient HIV status. (**D)** Detection of both MTBC and HIV-1 DNA in biopsy segments from open and CT-guided biopsy from PLWH, stratified by STB diagnostic group. Individual dots represent total DNA extracted per biopsy segment for either open (n=5/patient) or CT-guided biopsies (n=1/patient). MTBC+ = detection of (*rpoB* or *IS6110) and HIV-1+ (pol or gag)* X axis is MUTI patient ID. MUTI016 was on empiric anti-tuberculous therapy at the time for concurrent pulmonary TB with undetectable MTBC DNA yet detectable HIV-1 DNA. Correlation between HIV *pol* (**E**) and *gag* (**F**) copy numbers/million cells with *rpoB* gene copies per million cells in each biopsy segment. Correlation between patient HIV-1 VL in the blood and spinal biopsy (**G**) total detected *rpoB* copies **D**) and **E**) maximum *rpoB* copies per million cells detected across tested biopsy segments. HIV-1 gene copies/million cells for (**I**) *pol* and (**J**) *gag* in biopsy samples stratified by whether MTBC DNA (either *rpoB or IS6110*) was detected by ddPCR. P values were calculated with Mann-Whitney tests (A-C, I-J). Correlation coefficients and p-values were calculated with Spearman's test (E-H)). Lines show median values with interquartile range (IQR). Dots in all graphs coloured by STB diagnostic group, as per A-C. *GXPU: Xpert MTB/RIF Ultra; MTBC: Mycobacterium tuberculosis complex; TBCUL: MGIT TB culture. LOD: limit of detection.*